

XX. NEUROPHYSIOLOGY

Academic and Research Staff

Prof. Jerome Y. Lettvin	Dr. Edward R. Gruberg	Dr. Stephen G. Waxman
Dr. Michael H. Brill	Dr. Stephen A. Raymond	Paul A. Pangaro
	Dr. Donald Quick	

Graduate Students

Ian D. Hentall	Eric Newman	William M. Saidel
Bradford Howland	Louis L. Odette	Donald W. Schoendorfer
Lynette L. Linden		Marylou V. Solbrig

1. PERCEPTION OF COLOR

National Institutes of Health (Grant 5 TO1 EY00090-02)

Michael H. Brill

Even when we cannot directly see the light falling on an ensemble of objects, we tend to perceive object colors independently of the spectrum of this light. This color constancy may arise from comparisons of matte-reflected lights, but it may be facilitated by object highlights. We hope to develop a scheme whereby the human visual system might abstract illuminant-invariant object colors, subject to certain constraints.¹ Tangential to this problem is an investigation of the color cues accompanying the recognition of a translucent sheet partially eclipsing an ensemble of opaque objects.

References

1. M. H. Brill, "Color Vision: An Evolutionary Approach," Ph.D. Thesis, submitted to Department of Physics, Syracuse University, August 1974.

2. COLOR PERCEPTION IN THE VISUAL SYSTEM

National Institutes of Health (Grant 5 TO1 EY00090-02)

Lynette L. Linden

We have been concerned with looking at the information-handling aspects of the visual system, specifically in reference to color perception, as reported in Progress Report No. 116 (pp. 288-302). For example, considerations of information transmitted by receptor cells can be used to explain why color vision is at most a three-dimensional system. We shall continue to study similar theoretical issues, as well as to perform psychophysical experiments concerned with color perception.

(XX. NEUROPHYSIOLOGY)

3. STUDY OF VISUAL RECEPTOR MECHANISMS

National Institutes of Health (Grant 5 TO1 EY00090-02)

Eric Newman

The normally circulated retina of the intact and unanesthetized frog is being used to study mechanisms concerned with receptor cell physiology and adaptation. Intracellular recording from pigment epithelium cells has been conducted, and has shown that these cells hyperpolarize in response to light. The response has the same time course as the C-wave of the electroretinogram (ERG), in agreement with R. H. Steinberg's results from cat retina.¹ A detailed study of the time course of dark adaptation is in progress. Experiments investigating the affects of spatially and temporally different photopic stimuli on the B-wave of the locally recorded ERG are planned.

A light and electron microscopic investigation of the rod outer segments in the frog retina is being conducted with Edward R. Gruberg. The aim of this study is to determine whether the distribution of those discs in the rod outer segments attached to the plasma membrane change during dark adaptation.

References

1. R. Schmidt and R. H. Steinberg, "Rod-dependent Intracellular Responses to Light Recorded from the Pigment Epithelium of the Cat Retina," *J. Physiol.* 217, 71-91 (1971).

4. ADAPTIVE COLORATION OF FLATFISH

National Institutes of Health (Grant 5 TO1 EY00090-02)

William M. Sidel

In the estimation of this researcher, flatfish are second in sophistication only to the Cephalopod with respect to adaptive camouflage. The change in surface texture is initially rapid and is due to a visual stimulus. The mechanism at the cellular level appears comparable with that of other teleosts. We have focused on three separate aspects of flatfish camouflage:

- a. The dermal skin above the scales possesses a nervously innervated, stellate-shaped melanin-containing cell, the melanophore. Pigment granules within the cell migrate into and out of the cell body, and the processes depend upon the state of adaptation. We have focused on two aspects of this problem: a question posed many years ago and still unanswered about the number of neural-element types (one type for aggregation and/or one for dispersion), and the mechanism that induces the pigment granules within a process to line up as if on railroad tracks.
- b. The melanophores are not distributed uniformly throughout the fish. An irregular spatial distribution within the skin repeats itself over the entire skin. The strategy of texture matching appears to follow two principles: As the interradiation skin between the fin rays contains both a replica of the repetitive spatial unit and is transparent, the fins act to eliminate a discrete body contour by forming a "texture gradient." Examination of many other bottom fish species in a natural environment and in published works shows a similar feature that suggests a general contour-elimination principle whenever a superimposed texture attempts to hide within another. The body skin proper shows active modulation of these repetitive skin units, depending upon the bottom texture. We are actively seeking the principle of skin modulation used by the fish, but we have not yet been successful.

c. Under SCUBA examination the specific behavioral act of evading a predator has been identified in the local flatfish, Pseudopleuronectes americanus. This behavior depends solely on the visual appearance of the fish. A fish makes a sharp, right-angle turn from the path in which it is moving and descends quickly to the bottom. The success of this action depends solely on the right-angle turn which prevents tracking the animal to its new resting spot. Once tracking has been lost, the fish is effectively invisible. Other bottom fish that have been examined do not show this behavior.

5. HYDRODYNAMICS OF BIFURCATING BLOOD FLOW

National Institutes of Health (Grant 5 TO1 EY00090-02)

Michael H. Brill

It has been suggested by Jerome Y. Lettvin that pulsatile blood flow in a branching arteriole proceeds as follows: Each pressure pulse causes the blood to flow more in one branch than in the other, because of an instability at the stagnation point of the bifurcation. The branch preference is a random variable that resets itself with each pulse. We should like to observe the phenomenon in a variety of real situations, simulate it in a bifurcatory tube, and look for a theoretical explanation.

6. CHOLINERGIC SYSTEMS IN THE TECTUM

National Institutes of Health (Grant 5 TO1 EY00090-02)

Bell Telephone Laboratories, Inc. (Grant)

Edward R. Gruberg

We have demonstrated that there are two cholinergic inputs to the tectum, one retinal and one tegmental. The anatomical and dynamic relationship between the two systems is complex. We propose to use electron microscopy to show the distribution of cholinergic optic fibers by simultaneously marking optic fibers intracellularly with either procion brown or horseradish peroxidase, and acetylcholine postsynaptic receptor sites with horseradish peroxidase conjugated with α -bungarotoxin.

We hypothesize from our data that optic nerve lesions cause tectal sprouting of the tegmental system, but not vice-versa. This will be tested directly by sequential lesions and degeneration staining. From single-unit microelectrode recording we find units in the tegmental area that respond to visual stimuli similarly to tectal cells. The priority and correspondence of nucleus isthmus inputs to the tectum vs retinal inputs will be investigated.

7. MEASUREMENT OF HIGH-ORDER ABERRATIONS AND
PREDICTION OF EFFECTS ON VISION

Bell Telephone Laboratories, Inc. (Grant)

National Institutes of Health (Grant 5 TO1 EY00090-02)

Bradford Howland

The human eye is known to exhibit aberrations of a more complex sort than would be manifest, for example, in a poorly designed camera lens, since the elements comprising the optical train (i. e., corneal surface and lens) need not exhibit rotational symmetry. The measurement of high-order aberrations (i. e., those that cannot be corrected by ordinary spectacle lenses) and the prediction of their effects on vision can be greatly facilitated by a new aberroscope, an adaptation of a method originally developed

(XX. NEUROPHYSIOLOGY)

at the Research Laboratory of Electronics for testing camera lenses.¹

The new device forms a special test lens containing a grid and a crossed cylinder lens which fits in the trial lens frame of the refractionist or ophthalmologist. A point source of monochromatic light is viewed through it. The subject perceives an extended grid pattern, the distortions of which are directly identifiable with the first nine terms of the Taylor's expansion of the wave aberration surface. At present, drawings made by subjects are analyzed with the aid of a computer, and the degradation of the modulation transfer function and the percentile rating of each eye vis-a-vis the tested population are evaluated. We are working on a more advanced null-test method, using an electronic aberration generator by which the subject alone, or with the help of an operator, can adjust the controls so as to balance out the distortions of the perceived pattern.

Observations with the simpler test lens thus far have revealed a great variety of aberration patterns, and the results correlate with visual acuity in low light levels or in vision degraded by effects of corneal transplant.

References

1. Quarterly Progress Reports, Research Laboratory of Electronics, M.I.T., No. 77, April 15, 1965, pp. 383-389, No. 83, October 15, 1966, pp. 172-178; Appl. Opt. 7, 1587 (1968).

8. THEORY OF COLOR VISION

National Institutes of Health (Grants 5 RO1 EY01149-03 and 5 TO1 EY00090-02)
Bell Telephone Laboratories, Inc. (Grant)

Jerome Y. Lettvin, Marylou V. Solbrig, Jon W. Johnson

A variety of new and original "illusions" and tests have led to a relatively clear formulation of both the problem offered by color vision and what now seems to be a consistent theory for subjective color. The major difficulties that had to be overcome were (i) the dissection of the coordinate system of color from the classical chromaticity-brightness space, and (ii) the demonstration that color judgment on the image was local, not global. The present state of our work is to be issued soon as a prolegomenon.

One of our most interesting results has been the demonstration that global brightness is not at all directly related to the light intensity. This was achieved by showing that subjectively the perceived scene can be increasingly darkened continuously as the light everywhere in the image is continuously increased. This one observation removed the last difficulty from our preliminary theory.

In progress is a physiological experiment to verify the theoretical prediction that simultaneous contrast must be coded as for the colors seen by the ganglion cells. We are testing this first in pigeons, using the radiation to the lateral geniculate nucleus.

9. MECHANISMS OF PHOTORECEPTORS

National Institutes of Health (Grant 5 RO1 EY01149-03)
Bell Telephone Laboratories, Inc. (Grant)

Jerome Y. Lettvin

A two-conductance model of rod and cone outer segment, described in Quarterly Progress Report No. 112 (pp. 124-125), has become more plausible with newer results from other laboratories. Our current hypothesis proposes that signal amplification and shaping takes place by the operation of the ellipsoid. We have some evidence for this process, but it is now ambiguous, and we shall continue to pursue the matter.

10. MEMBRANE PROCESSES

National Institutes of Health (Grant 5 RO1 EY01149-03)

Bell Telephone Laboratories, Inc. (Grant)

Stephen A. Raymond

During the past year, we have defined a role for nerve threshold shifts in determining the periodic nature of intermittent conduction in axons. The influence of temperature on activity-dependent threshold shifts is very strong for active nerve fibers. Threshold changes are also pronounced following application of a variety of drugs. These studies lead us to a picture of the nervous system in which conduction along the axons is contingent not only on the local past history of the fiber, but also on the local fluctuations of pH, glucose, oxygen, CO₂, ions, temperature, and hormones. This perspective admits of a nervous system that is rather densely coupled by "metabolic" as well as by electrical variables. As we have tried before to reassure ourselves, this need not imply that such a codependence of a variety of channels will result in a degradation of information-handling capacity or reliability.

These drug effects on threshold and on conduction of impulses at regions of low conduction safety have not been studied well and are not well understood. During the coming year, we intend to direct our attention to the effects of a few of these drugs. We have already experimented with ethanol, strychnine, acetylcholine, CO₂ and N₂O. In each case the drugs have had a singular effect on the threshold at concentrations roughly equivalent to clinically significant doses. Our understanding of the effects is limited in part by the lingering questions about activity-dependent threshold curves. Thus we intend to continue our recent work with ouabain and ion pump inhibitors to try to parse the role played by such pumps in generation and recovery from threshold depression at high impulse rates. Our work thus far implies strongly that the pump is solely responsible for building and recovery of depression. It is likely that temperature changes manifest themselves primarily by affecting the rate of an ion pump. By using Ringer's solutions of varying ionic composition, the impetus behind the transient superexcitability phase should become clearer. We believe that for the most part it is due to a lingering extracellular increase in potassium ion concentration following the impulse. Some of the drug effects are complex, and it is essential to know the basic mechanisms relating threshold to activity before they can be interpreted.

Finally, we are eager to continue research on the performance of axon trees as information-handling devices. Our studies helped to develop expectations for the relation between invadability in axons and impulse patterns. We have tested several possible modes of operation for a model axon, but have not yet discovered an appropriate formulation for the meaning of a pattern and an interpretation of the filter output.

11. CODING PROPERTIES OF SUBSTANTIA GELATINOSA CELLS
IN THE CAT'S SPINAL CORD

Bell Telephone Laboratories, Inc. (Grant)

Ian D. Hentall

Extracellular recording from this region has revealed a hitherto unreported class of cells, defined by their time pattern of nerve impulses. Previous expectations of the activity of these cells (based on an analysis of current source density following dorsal root stimulation and the transection of Lissauer's tract¹) were that averaged frequencies follow the time course of dorsal root potentials, and that the A-fibers have an influence

(XX. NEUROPHYSIOLOGY)

that is opposite to that of C-fibers. Also, lesions of Lissauer's tract in monkeys show delays of several days before causing an abrupt change in skin sensation, which leads to an idea of substantia cells as temporal integrators of cutaneous stimuli.²

We have now discovered that the basic response pattern of these cells is a burst of activity from an otherwise silent unit, lasting several seconds and having a progressive slowing of frequency. The following rules appear to govern the occurrence of such a burst, which is usually an "all-or-none" event:

a. It may occur without active stimulation of the skin by the experimenter. The probability of this event occurred after the receptive field had been strongly or persistently stimulated some minutes previously.

b. Touching the skin with an electromechanical probe elicits a burst, but not consistently; the factors governing its occurrence have not been discovered. A second touch to the same area after a burst has begun will erase the remainder of the activity. When one area of skin has become ineffective, touching a second nearby spot will cause an initial burst.

c. Single electrical pulses (0.1 ms) delivered through needles in the skin also produce bursts with a probability of less than one. Any stimulus strength above threshold exhibits the same basic effect. This demonstrates that A- and C-fibers are not acting in opposition, and the fact of the burst duration lasting longer than the mechanical stimulus is not due to slow mechanical factors in the skin.³

Units that have been held for more than 30 min, and whose receptive fields have been subjected to strong mechanical or thermal stimulation, display a steady resting frequency around 10 impulses per second. They also have a burst response to touch, and in this case the number of impulses in a burst is inversely related to the previous steady firing frequency.

There are, therefore, suggestive correspondences between the single-unit record and studies with other methods. The observed firing patterns indicate a multiplexing of information on long- and short-term skin history, which is similar to that seen in the frog's optic nerve. A salient feature of substantia organization is the interconnectedness of its cells; when this is coupled with the "spontaneous bursting behavior" and the non-repeatability of the effects of identical stimuli delivered at well-spaced intervals, a model involving a reverberatory network for long-period integration becomes attractive. A full model has not yet been attempted, since this list of general principles is incomplete, and the synaptic connections of this region are unknown.

References

1. P. D. Wall, "The Origin of a Spinal Cord Slow Potential," *J. Physiol. (London)* 164, 508-526 (1962).
2. D. Denny-Brown, E. J. Kirk, and N. Yanagisawa, "The Tract of Lissauer in Relation to Sensory Transmission in the Dorsal Horn of the Spinal Cord in Macaque Monkey," *J. Comp. Neurol.* 151, 175-200 (1973).
3. S-H. Chung, S. A. Raymond, and J. Y. Lettvin, "Multiple Meaning in Single Visual Units," *Brain Behav. Evol.* 3, 72-101 (1970).

12. NERVE MEMBRANE MODELS

Bell Telephone Laboratories, Inc. (Grant)

Louis L. Odette

Analysis and synthesis of electronic analog models of nerve membrane is in progress. With this background we shall explore the relations between the models (considered as equivalent representations of the Hodgkin-Huxley equations) and physical representations of the nerve membrane.

13. DESIGN AND CONSTRUCTION OF ARTIFICIAL VOCAL CORDS

Bell Telephone Laboratories, Inc. (Grant)

Donald W. Schoendorfer

Three major prosthetic vocal-cord designs have been tested in vivo, the duck-call larynx, the starling larynx, and the Japanese reed. These three designs employ the external reed fistula technique of speech rehabilitation following laryngectomy. Following this method, a skin fistula between the external neck and the pharynx directs the sound produced by the external larynx to the vocal tract of the laryngectomized patient. The fistula is a tube of 5/16" OD and from 3 to 20 cm long.

The duck-call larynx is a scaled-down version of a common duck call striking reed with certain design variations to help smooth the frequency spectra and to copy the spectra of normal vocal cords. The starling larynx is a thin rubber tube (0.010" wall thickness) in a reduced pressure chamber. When the tension and pressure differential between the inside and outside of the tube is critically controlled, the tube will oscillate between open and collapsed states and produce suitable frequency spectra. The Japanese reed, a device currently used by some laryngectomized patients, has certain disadvantages that will be avoided in other designs.

Spectra of sentences spoken by patients using these different artificial cords show certain constant formants of energy that appear for all voiced sounds. We believe these "masking" formants are created by radiation from the external source itself and from the spectrum of the fistula tube which is superimposed on the vocal tract's spectra.

Effort is now being spent to miniaturize the artificial vocal cords so that they can be placed at the very end of the fistula tube. The cords will then lie under the skin in the neck and radiation will be diminished. The downstream length of tube needed to direct the sound from the cords to the vocal tract will be negligible. The patient's speech should then be much more intelligible.

14. STUDIES ON THE DIFFERENTIATION OF AXONS

National Institutes of Health (Grants NS 12307-01 and 1 KO4 NS00010)

Bell Telephone Laboratories, Inc. (Grant)

Stephen G. Waxman, Donald Quick

We are attempting to study the developmental mechanisms that determine specificity in neuroglial relationships, using the model system provided by the electrocyte axons in the gymnotid *Sternarchus albifrons*. These axons exhibit a high degree of regional differentiation in the structure of nodes of Ranvier. The nodes in two areas along the fiber are enlarged and do not generate spikes. Since these specialized nodes always occur in the same regions, we hope to address the questions of how Schwann cells

(XX. NEUROPHYSIOLOGY)

recognize axons, and how they match various aspects of myelin sheath morphology to the design requirements of the axon with the use of this system. Histochemical and ultrastructural studies of the development of these axons are in progress.

15. STUDIES ON IMPULSE CONDUCTION ALONG CENTRAL AXONS

National Institutes of Health (Grants NS 12307-01 and 1 KO4 NS00010)
Bell Telephone Laboratories, Inc. (Grant)

Harvey Swadlow, Stephen G. Waxman

[Dr. Swadlow's research was performed at the Eye Research Institute of the Retina Foundation, Boston. His current address is the Department of Psychology, University of Western Ontario, London, Ontario, Canada.]

We are studying conduction properties of the axons of binocular visual neurons in the corpus callosum of the rabbit. Previous studies by several workers, including Eric Newman and Stephen A. Raymond of this laboratory, have shown variations in threshold and conduction velocity for peripheral axons. Our data indicate that such structure-function relations as exist for central axons may not be invariant, since the conduction velocities of rabbit callosal axons vary with the history of impulse conduction along the fiber. Increases and decreases occur in conduction velocity. Constant latency, therefore, does not constitute a necessary condition for identification of antidromically activated neurons, and variable latency does not constitute a sufficient condition for identification of synaptically activated neurons. Furthermore, interspike intervals will not be invariant for a given callosal neuron but will depend on where the impulse activity is measured. We have observed latency variation (total range of latency increases and decreases) as large as several milliseconds in the antidromic activation of callosal neurons. Since some postsynaptic neurons are tuned to fine differences in presynaptic interspike intervals, latency variations of this magnitude, occurring systematically as a result of prior activity of the axon, may have significance for coding and decoding of neural messages. We are now extending our analysis to trains of impulses and studying the ultrastructure of these axons.

16. PATHOPHYSIOLOGICAL STUDIES ON PERIPHERAL
NEUROPATHIES

National Institutes of Health (Grants NS 12307-01 and 1 KO4 NS00010)
Bell Telephone Laboratories, Inc. (Grant)

Stephen G. Waxman, Michael H. Brill, Jerome Y. Lettvin

In collaboration with Norman Geschwind, of Harvard Medical School, and Thomas D. Sabin, of Boston City Hospital, we have begun a series of investigations that attempt to relate neuronal pathophysiology to clinical symptomatology in the peripheral neuropathies. Our initial studies are aimed at defining the prerequisites for distal sensory loss and paresthesia. We have developed a set of random-distribution models that reproduce the clinically observed reduction in length along which sensory conduction proceeds normally. These models are based on conduction block, coherence loss, and weak interactions between fibers. They demonstrate that randomly distributed axonal dysfunction provides a sufficient, though not necessary, condition for distal sensory deficit. These models also predict a marked reduction in the length along which conduction of sensory messages proceeds normally, with small increases in the probability of axonal

dysfunction, and provide a possible correlate for the rapid clinical progression of some neuropathies.

17. EXPERIMENTAL NEUROPATHOLOGICAL STUDIES

National Institutes of Health (Grant NS 12307-01 and 1 KO4 NS00010)

Bell Telephone Laboratories, Inc. (Grant)

Stephen G. Waxman

We continue to study the pathology of a number of neurological diseases, particularly those affecting axons in the peripheral and central nervous system. Our recent studies on a case of disseminated subpial demyelination suggests a selective susceptibility of the subpial axons to demyelination in some patients. We are also studying the effects of several toxins and antimetabolites on the ultrastructure of the nervous system. Our future studies include investigations on altered conduction properties in multiple sclerosis, in both animal models (experimental allergic encephalomyelitis) and humans (evoked potential studies).

XX. NEUROPHYSIOLOGY

A. CHOLINERGICITY IN THE OPTIC NERVE AND TECTUM OF THE FROG

National Institutes of Health (Grant 5 TO1 EY00090-02)
Bell Telephone Laboratories, Inc. (Grant)

Edward R. Gruberg

In Progress Report No. 116 (pp. 266-273) we showed that there was high acetylcholinesterase (AChE) activity in areas with optic fiber terminals and moderate AChE activity along the optic tract and optic chiasm, while in the outer half of the tectum where all retino-tectal fibers end there was high cholineacetyltransferase (CAT) activity. Dr. John Freeman, of Vanderbilt University, had demonstrated that α -bungarotoxin (α BT), which selectively and irreversibly binds to the acetylcholine receptor protein, binds in the outer half of the toad tectum. Also, "monosynaptic" optic nerve fiber/tectal cell synapses were blocked by α BT. Taken collectively, this evidence suggested that acetylcholine (ACh) is an optic nerve fiber neurotransmitter.

But it has been argued that another nonretinal system of cholinergic fibers could exist that has a similar distribution and is interposed between optic fiber terminals and tectal cells. This could account logically for all of the results.

If the optic nerve fibers are cholinergic, CAT is presumably synthesized in the ganglion cell bodies of the retina and transported down the nerve. So there should be a way of parsing out which of the two systems is cholinergic. As a way of testing this, two sets of related experiments have been carried out: (a) By ligating the optic nerve, ACh synthesis should increase in the segment of the nerve on the eye side of the ligation and decrease on the other side. (b) If the optic fibers are cholinergic, ACh synthesis in the tectum should decrease in the deafferented tectal lobe compared with the normally innervated lobe (each tectal lobe receives retinal fibers only from the contralateral eye).

In the course of these experiments choline (Ch) uptake and the effects of anticholinesterases were also explored.

The methods used have been described in detail in Progress Report No. 116 (pp. 266-273). In all experiments but one the leopard frog Rana pipiens was used. The distribution of optic fibers and AChE activity and the high tectal CAT activity in Rana is essentially the same as that in Bufo. Tissue was incubated overnight in L-15 tissue-culture medium deficient in choline to which ^{14}C -methyl choline chloride was added. The tissue was then rinsed in cold medium and homogenized. Aliquots were removed for Lowry total-protein assay. The remainder was spotted on electrophoresis paper and co-electrophoresed with unlabeled choline and acetylcholine. The paper was dried, stained with iodine and cut up, and radioactivity was measured in a scintillation counter.

(XX. NEUROPHYSIOLOGY)

In the nerve-block experiments the animals were anesthetized, and the optic nerve was exposed by going through the upper mouth. The nerve was either ligated or cut. Table XX-1 summarizes the results. In all cases there was an increase in optic nerve ACh synthesis on the side proximal to the eye relative to both the control nerve and, where obtainable, to the segment of the nerve proximal to the brain. This is consistent with the hypothesis that optic fibers are cholinergic.

Table XX-1. Comparison of acetylcholine synthesis in ligated or cut optic nerves and in their contralateral normal optic nerves.

Material	E/N	E/B
1. optic nerve cut 28-day survival	4.5	—
2. optic nerve ligated 1-day survival	1.87	too small for Lowry
3. optic nerve ligated 2-day survival	1.48	1.55
4. optic nerve ligated 8-day survival	1.63	5.15

E is ACh synthesis/protein in segment of optic nerve proximal to eye.
B is ACh synthesis/protein in segment of optic nerve proximal to brain.
N is ACh synthesis/protein in normal (contralateral) optic nerve.

Before studying ACh synthesis in the deafferented tectum, the time course of ACh synthesis and Ch uptake was determined for a normal tectum. To a first approximation ACh synthesis and Ch uptake are linear over the time of incubation (Fig. XX-1).

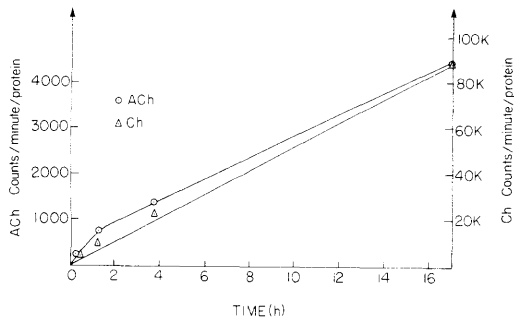


Fig. XX-1.
ACh synthesis and Ch uptake
vs time.

We then compared ACh synthesis in the deafferented tectum with that in the normal tectum (Table XX-2).

Table XX-2. Comparison of ACh synthesis in normal and optic nerve deafferented tectal lobes.

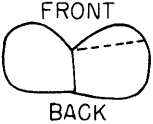
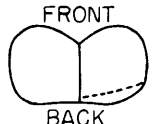
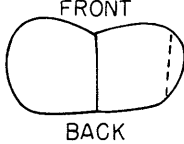
Material	D/N
Toad enucleation 28-day survival	1.49
Frog optic nerve cut 28-day survival	1.30
Frog 1-day ligation	1.15
Frog 2-day ligation	1.15
Frog 8-day ligation	1.05

D is ACh synthesis/protein in deafferented tectum.

N is ACh synthesis/protein in normal (contralateral) tectum.

In every case, ACh synthesis is higher on the deafferented side. These results suggest two possibilities: either the optic fibers are not cholinergic, or there is another cholinergic system which increases its CAT output (by higher CAT synthesis and/or sprouting new fibers) in response to degeneration or inactivity of optic nerve fibers. We suggest that the ligation experiments are a strong confirmation for optic fiber cholinergy.

Table XX-3. Comparison of ACh synthesis in normal and lesioned tectal lobes.

Material (showing tectal surfaces)	D/N
	1.21
	1.30
	.67

D is ACh synthesis/protein in deafferented tectum.

N is ACh synthesis/protein in normal (contralateral) tectum.

(XX. NEUROPHYSIOLOGY)

As a start in determining which other tectal system could be cholinergic, we made a series of electrolytic lesions (25 μ A, 10 s) in three animals, blocking inputs and outputs respectively from the front, side and back of the tectum. Electrolytic lesions coagulated tissue without disturbing blood flow at the tectal surface. The animals were kept for seven days until tissue incubation. The results are summarized in Table XX-3. Only the brain with tectal lesions running laterally showed a decrease in ACh synthesis. Note that the lateral lesion interrupted optic fibers entering from the lateral optic tract. To locate other possible cholinergic inputs we are making lesions in nuclei which project to the tectum and enter laterally. Another possibility is that tectal cells are cholinergic.

Presumably most ACh synthesis occurs at nerve terminals where ACh is released, hydrolyzed by AChE to choline, and the choline is taken up again presynaptically, and resynthesized to ACh by CAT. Table XX-4 gives a comparison of CAT activity and choline uptake of the optic nerve to the tectum and to the pallium. The latter is in the dorsal

Table XX-4. Comparison of choline uptake and ACh synthesis in normal tectum, pallium, and optic nerve.

	N_{T_A}/N_{N_A}	N_{T_A}/N_{P_A}	N_{N_C}/N_{T_C}	N_{N_C}/N_{P_C}
Frog 1	6.2	—	2.4	—
Frog 2	11.0	—	1.7	—
Frog 3	3.9	17.1	6.3	18.0
Frog 4	4.5	—	4.1	—

N_{T_A} is ACh synthesis/protein normal tectum.
 N_{N_A} is ACh synthesis/protein normal optic nerve.
 N_{P_A} is ACh synthesis/protein pallium.
 N_{T_C} is Ch uptake/protein normal tectum.
 N_{N_C} is Ch uptake/protein normal optic nerve.
 N_{P_C} is Ch uptake/protein normal pallium.

forebrain and does not show significant AChE activity. The optic nerve shows the highest uptake of choline and is intermediate in ACh synthesis. Note that CAT activity as measured in these experiments is also a function of choline uptake.

Finally, Table XX-5 summarizes the effect of anticholinesterases (eserine 10^{-4} M; BW284C51 10^{-4}) on ACh synthesis and choline uptake.

The decrease in synthesis of ACh is correlated with a decrease in the uptake of

Table XX-5. Effect of 2 anticholinesterases, eserine and BW284C51 on ACh synthesis and choline uptake.

Anticholinesterase	N_{N_A}/N_{A_A}	N_{N_C}/N_{A_C}
10^{-4} M Eserine	1.8	1.6
10^{-4} M BW284C51	2.08	2.06

N_{N_A} is ACh synthesis/protein normal optic nerve.
 N_{A_A} is ACh synthesis/protein optic nerve
+ 10^{-4} M anticholinesterase.
 N_{N_C} is Ch uptake/protein normal optic nerve.
 N_{A_C} is Ch uptake/protein optic nerve
+ 10^{-4} M anticholinesterase.

choline. This implicates choline uptake as rate limiting on ACh synthesis.

In conclusion, additional evidence has been obtained suggesting that acetylcholine is an optic fiber neurotransmitter, and that the tectum probably has at least another cholinergic system.

B. PHYSICAL FOUNDATIONS OF THE PERCEPTION OF ACHROMATIC TRANSLUCENCY

National Institutes of Health (Grant 5 TO1 EY00090-02)

Michael H. Brill

Given the arrangement of gray matte papers shown in Fig. XX-2, with reflectances A , A_1 , B_1 and $B \in [0, 1]$, it is sometimes possible to perceive areas A_1 and B_1 as a single translucency over A and B . This illusion depends on the reflectances. If the two interior areas are white and black, for example, the illusion will not work. Metelli¹ has proposed constraints on the reflectances based on a psychophysical model of the

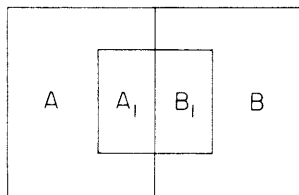


Fig. XX-2.

Four matte papers brought together to simulate a translucent sheet A_1B_1 over areas A and B .

perception of translucency, and Stefanescu² has discussed some of the model's ramifications. This report will examine the model and its relationship with the constraints on the apparent reflectances attainable by a real translucent sheet eclipsing two matte papers. The symmetry of the problem will be exploited by setting $B > A$.

1. Metelli's Theory of Color Scission

When a sectored disk is spun very fast, its colors fuse into a spatially weighted average color. Suppose a sectored disk has fraction f of its area transparent and a fraction $(1-f)$ opaque with reflectance t . Clearly $f, t \in [0, 1]$. If this disk is spun over matte reflectors A and B as in Fig. XX-3, the apparent reflectances A_1 and B_1 will be given by

$$A_1 = fA + (1-f)t$$

$$B_1 = fB + (1-f)t.$$

Metelli proposes that since we tend to see the spinning disk as translucent, the rules governing the perception of translucency evolve from trying to infer an f and a t from four reflectances arranged as in Fig. XX-2, as if they had arisen from a disk spinning over two matte papers. This "color scission" corresponds mathematically to solving the reflectance equations for f and t .

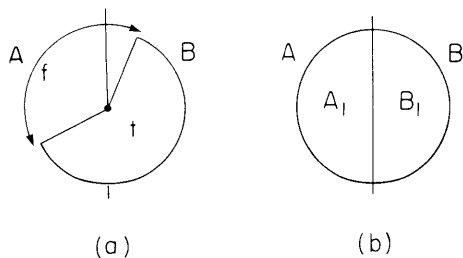


Fig. XX-3

Sectored disk of Metelli's color scission model. (a) Not spinning. (b) Spinning.

In order for an ensemble $A_1 B_1$ to be replaceable by such a sectored disk over A and B , the inferred values f and t must belong to $[0, 1]$. Also, f cannot be 0, for then there would be no border between A_1 and B_1 , and opacity, rather than translucency, would be seen.

We now eliminate f and t from the phrasing of these criteria:

(i) $f > 0$ is equivalent to $\frac{B_1 - A_1}{B - A} > 0$. Since $B > A$, this means $B_1 > A_1$.

(ii) $f \leq 1$ is equivalent to $B_1 - A_1 \leq B - A$.

(iii) $t \geq 0$ is equivalent to $\frac{BA_1 - AB_1}{(B-A) - (B_1 - A_1)} \geq 0$. From (ii), the denominator is non-

negative, so $\frac{B}{A} \geq \frac{B_1}{A_1}$.

(iv) Similarly, $t \leq 1$ is equivalent to $BA_1 - AB_1 \leq (B-A) - (B_1 - A_1)$.

Can these inequalities in reflectance be assessed by a visual system that has access only to reflected light? Since the eye receives an inseparable product of illuminant intensity and reflectance, scaling all reflectances in Fig. XX-2 by the same factor must be indistinguishable from scaling the light intensity by this factor. Therefore, we cannot unambiguously assess inequalities involving reflectances unless these inequalities are scale-invariant: that is, multiplying all reflectances by the same number should not make a change in whether or not the rules are obeyed. Although (i)-(iii) are scale-invariant, (iv) is not. For example, the ensemble $\{B_1 = .4, B = .3, A_1 = .2, A = .01\}$ obeys all these rules, but scaling up these numbers by 1/.4 causes rule (iv) to be violated. Thus there is no way to decide on the basis of reflected light alone whether a given reflectance ensemble could have arisen from Metelli's spinning disk paradigm. Metelli talks only about the scale-invariant rules (i)-(iii), which provide a way to reject some but not all ensembles that could not have arisen from the spinning disk paradigm.

2. Physical Constraints on Translucency

We now address the question of the relation of Metelli's rules to physical translucency. Translucent materials are commonly idealized as volume scatterers. A thin ideal translucent sheet transmits a fraction c of light and diffusely reflects a fraction r at each pass (where r, c , and $(r+c) \in [0, 1]$).

From the Kubelka-Munk analysis of colorant layers (see Wyszecki and Stiles³), a translucent sheet lying on top of matte surfaces with reflectances A and B will give rise to apparent reflectances

$$A_1 = r + \frac{c^2}{\frac{1}{A} - r}, \quad B_1 = r + \frac{c^2}{\frac{1}{B} - r}.$$

If we add to these constraints on r and c by ruling out the cases of opacity ($c = 0$ or $r = 1$) and perfect transparency ($r = 0, c = 1$), the model can be summarized as follows:

$$\left. \begin{array}{l} \text{(a) } A_1 = r + \frac{c^2}{\frac{1}{A} - r} \\ \text{(b) } B_1 = r + \frac{c^2}{\frac{1}{B} - r} \\ \text{(c) } 0 < c < 1 \\ \text{(d) } 0 \leq r < 1 \\ \text{(e) } r + c \leq 1 \end{array} \right\} \text{P1}$$

(XX. NEUROPHYSIOLOGY)

We remove r and c from the phrasing of these rules and get the equivalent statement P2 (see Appendix 1):

$$\left. \begin{array}{l} \text{(a) } B_1 > A_1 \\ \text{(b) } \frac{B_1}{A_1} \leq \frac{B}{A} \\ \text{(c) } A_1 - B_1 + \frac{1}{A} - \frac{1}{B} > 0 \\ \text{(d) } (B-A)(1+A_1B_1-2A_1) \geq (B_1-A_1)(1+AB-2A) \end{array} \right\} \text{P2}$$

As is the case for Metelli's spinning disk paradigm, lack of scale-invariance forbids P2 from being an assessable set of rules. (The previous counterexample can be used to illustrate the point.) A set of scale-invariant rules P3, however, is implied by P2 (see Appendix 2):

$$\left. \begin{array}{l} \text{(a) } B_1 > A_1 \\ \text{(b) } \frac{B_1}{A_1} \leq \frac{B}{A} \\ \text{(c) } B - A > B_1 - A_1 \end{array} \right\} \text{P3}$$

These are Metelli's scale-invariant rules (i)-(iii), minus the case of perfect transparency. Since a physical translucency and a spinning disk share these constraints on apparent reflectance, it is not surprising that one should be mistaken perceptually for the other. But both paradigms give rise to rules that are not scale-invariant and therefore cannot be assessed by any visual system. Perhaps, then, the perception of translucency involves more than the cues of figure and color that heretofore have been used to explain it.

Appendix 1

Proof That P1 Is Equivalent to P2

I. $P1 \rightarrow P2$

$$\text{(a) From P1(a) and P1(b), } B_1 - A_1 = \frac{c^2(B-A)}{\left(\frac{1}{B} - r\right)\left(\frac{1}{A} - r\right) AB} > 0, \text{ as long as } B > A.$$

Thus $B_1 > A_1$.

(b) From P1(a) and P1(b), $c^2 = \left(\frac{1}{A} - r\right)(A_1 - r) = \left(\frac{1}{B} - r\right)(B_1 - r)$. In order for c to be real and nonzero,

$$r = \left(\frac{A_1}{A} - \frac{B_1}{B} \right) / \left(A_1 - B_1 + \frac{1}{A} - \frac{1}{B} \right) < A_1.$$

If the numerator of r is less than zero, then the inequality is equivalent to $A_1 B > 1$, which is never satisfied for $A_1, B \in [0, 1]$. Therefore, the numerator of r must be nonnegative, whence $\frac{B}{A} \geq \frac{B_1}{A_1}$.

(c) Since r and its numerator are nonnegative, its denominator is positive:

$$A_1 - B_1 + \frac{1}{A} - \frac{1}{B} > 0.$$

(d) From P1(e), $r + c \leq 1$; equivalently, $(1-r)^2 \geq c^2 = (A_1 - r) \left(\frac{1}{A} - r \right)$, whence

$$\frac{A_1}{A} - 1 \leq r \left(\frac{1}{A} + A_1 - 2 \right).$$

Substituting the expression for r in (b), we get

$$(B-A)(1+A_1 B_1 - 2A_1) \geq (B_1 - A_1)(1+AB-2A).$$

II. P2 \rightarrow P1

The "whence" in I(d) is actually an equivalence, given that r is defined as in I(b) and $c^2 = (A_1 - r) \left(\frac{1}{A} - r \right)$. Thus $r + c \leq 1$. Since c always appears in the square, we may presume $c \geq 0$, and since both numerator and denominator of r are nonnegative, it follows that $r \geq 0$. The case $c^2 = 0 = (A_1 - r) \left(\frac{1}{A} - r \right) = (B_1 - r) \left(\frac{1}{B} - r \right)$ demands $A_1 = B_1 = r$, which is precluded by P2(a). Thus $c \neq 0$. Similarly, $c = 1, r = 0$ implies $c^2 = 1 = A_1/A = B_1/B$. This violates P2(c). The case $r = 1$ is precluded by noting from I(d) that $\frac{A_1}{A} - 1 \leq r \left(\frac{1}{A} + A - 2 \right)$ is impossible if $r = 1$ and $1 \geq B > A$.

Appendix 2

Proof That P2 Implies P3

(a) and (b) P2(a) and P2(b) are identical to P3(a) and P3(b).

(c) If $A_1 < A$, then P2(b) becomes $\frac{B-A}{A} \geq \frac{B_1 - A_1}{A_1} > \frac{B_1 - A_1}{A}$, whence $B-A > B_1 - A_1$.

If $A_1 = A$, then there is perfect transparency, which has been ruled out.

If $A_1 > A$, denote two subcases:

Subcase 1. If $A_1 B_1 + 1 - 2A_1 < AB + 1 - 2A$, then P2(d) implies P3(c) directly.

Subcase 2. If $A_1 B_1 + 1 - 2A_1 \geq AB + 1 - 2A$, then $\frac{A_1}{A} \leq \frac{2-B}{2-B_1}$. Since $A_1 > A$, it follows

(XX. NEUROPHYSIOLOGY)

that $1 < \frac{2-B}{2-B_1}$, whence $B < B_1$. From P2(b), $\frac{B_1}{B} \leq \frac{A_1}{A} \leq \frac{2-B}{2-B_1}$, whence $B_1(2-B_1) \leq B(2-B)$. But this is incompatible with $B < B_1$ because $B(2-B)$ is an increasing function of B over the interval $[0, 1]$. Thus Subcase 2 does not occur.

References

1. F. Metelli, "The Perception of Transparency," Scientific Am., Vol. 230, pp.90-98, April 1974.
2. D. Stefanescu, "Transparency," Working Paper 107, M. I. T. Artificial Intelligence Laboratory, July 1975.
3. G. Wyszecki and W. S. Stiles, Color Science (John Wiley and Sons, Inc., New York, 1967).

C. COLOR GAMUT THEORY IN THE ASSESSMENT OF LIGHTS
AND PIGMENTS

National Institutes of Health (5 TO1 EY00090-02)

Michael H. Brill, Bradford Howland

1. Introduction

The present wide variety of artificial illuminants has motivated the search for an index of how well a spectrum of light renders object colors. This search requires an understanding of the reception of light in the eye. Since the eye sees three qualities of reflected light, the color of an object can be represented as a point in a linear three-space called tristimulus space. The location of a point is determined by the energy spectrum of the illuminant, the spectral reflectance of the object, and the assumed spectra of the three types of photosensor in the eye. Typically, an illuminant index uses several standard pigments, and catalogs some aspect of the arrangement of points that they engender in a tristimulus space under a given illuminant. Some examples are the Color Rendering Index,¹ the Flattery Index,² and Thornton's Color Discrimination Index.³

Thornton's index³ has a particularly intuitive appeal. He projects the points representing 8 Munsell colors onto a uniform chromaticity plane, in which colors are more discriminable the greater their distances from one another. His index is simply the area of the polygon generated by these points. Its name derives from the tendency of colors to be more distinguishable when they occupy a larger area in the uniform chromaticity plane.

In the hope of arriving at a rule of thumb for ordering illuminants aesthetically (independently of color discrimination), we have extended Thornton's notion of color gamut

in two ways.

First, Thornton's standard Munsell pigments have approximately the same luminosity under most lights, so they are not representative of the full set of pigment colors encountered in an artist's palette. Pigments with differing luminosities require 3 dimensions to express their color gamut. This suggests a more general definition of color gamut as the volume of the polyhedron generated by a specified set of pigments in a tristimulus space, with a given illuminant. This measure of color gamut allows us not only to order illuminants, given a standard pigment set, but also to order pigment sets for a given illuminant.

Second, we would like our index to characterize the spectrum of a light independently of its intensity. Thornton's index does this naturally, since the chromaticity plane conveys only intensive color information. In three-space, however, normalization is required. In this regard, the ideas of von Kries⁴ and of Land and McCann⁵ are helpful: When objects are looked at under a colored light for some time, a white object tends to appear white even though it reflects the ambient light. Accordingly, we represent this chromatic adaptation (or normalization) in tristimulus space by stipulating that white occupy the point (1, 1, 1), and the coordinates of the other colors are scaled accordingly.

2. Program for Computing Normalized Volumes in Tristimulus Spaces

Given an illuminant spectrum, pigment spectral reflectances, and the spectral curves defining tristimulus space, we have developed a computer program to calculate color gamuts. The program operates in two stages.

The first stage is identification of the limit color points, which are the vertices of the limit polyhedron. Each pigment from the set of colors under consideration is entered first as a point in the tristimulus space. These points are then sequentially tested by passing a plane through a given candidate point. Then lines are drawn connecting all points on one side of this plane with all points on the other side, and the intersection points of these lines with the plane generate a convex limit polygon. If the candidate point lies outside this polygon, it must be a limit point.

The second stage is calculation of the volume of the limit polyhedron. The space is sectioned by 10 or more equally spaced planes. The limit points on both sides of each plane are connected as before, and the area of the convex limit polygon is determined. (The limit points of this polygon are identified by comparing distances from its centroid as the polar angle is scanned about this centroid.) These areas are multiplied by the interplane spacing and summed to get the volume of the solid.

3. Computed Color Gamuts

We computed gamuts for two sets of hypothetical spectral sensitivities in the eye, those of Judd⁶ and of Vos and Walraven.⁷ We used two sets of pigments: Thornton's

Table XX-6. Gamut characteristics of 9 illuminants.

Illuminant	Symbol	Thornton's Gamut Area $\times 2 \times 10^4$	Gamut Volume $\times 10^4$			Correlated Color Temperature (°K)
			Judd Space	Vos-Walraven Space		
		Munsell Pigments	Munsell Pigments	Munsell Pigments	Artist Pigments	
Maximum Gamut Fluorescent*	MG	212	137	194	915	16416
Illuminant C	C	100	66	99	527	6740
Prime Color Fluorescent* (Cool White)	PC	90	88	129	664	4237
Standard Daylight Fluorescent*	DF'	73	52	79	438	6549
Deluxe Mercury*	DM	56	69	98	489	3610
Illuminant A	A	53	88	125	622	2854
Standard Warm White Fluorescent*	WW	45	68	96	487	2907
High-Pressure Sodium	Na	18	56	77	393	
Gold Fluorescent*	GF	0	14	15	100	2418

*Spectral information provided by W. A. Thornton.

set of 8 Munsell pigments, together with white and black, and a set of 35 artist pigments (spectral reflectances⁸ obtained from Barnes) augmented by black and white. Using the nine illuminants listed in Table XX-6, we found that the gamut volumes for Thornton's Munsell pigments are proportional to the gamuts for artist pigments, when using either Judd or Vos-Walraven color curves.

Next, we made a comparison between our color volume and Thornton's gamut area, for each of the nine illuminants listed in Table XX-6 and for several others (see Fig. XX-4). The extremes of the gamut are in agreement: The lamp that maximizes

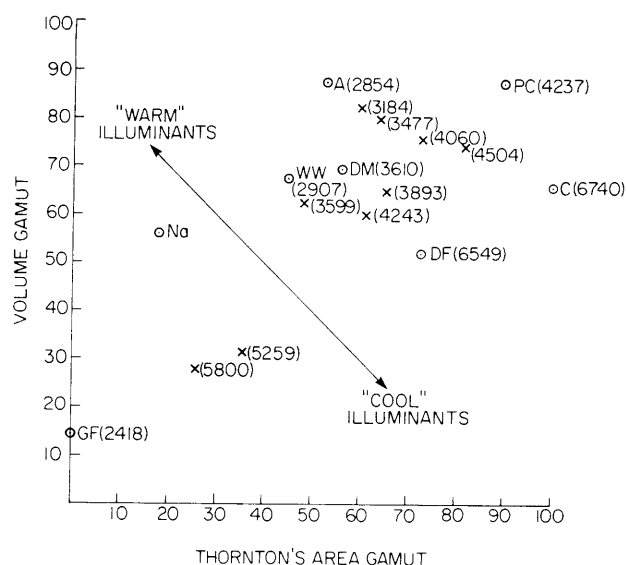


Fig. XX-4. Volume vs area gamut for various illuminants. Abscissa: $2 \times 10^4 \times$ Thornton's gamut area. Ordinate: $10^4 \times$ gamut volume for Munsell pigments in Judd space. Correlated color temperatures ($^{\circ}$ K) for each illuminant in parenthesis. ● Data points for illuminants in Table XX-6. ⊗ Other illuminants. Spectral data for these additional illuminants have been kindly furnished by W. A. Thornton.

Thornton's gamut area also gives a large volume, and the gold fluorescent light, whose spectrum cuts off below 520 nm, scores nearly zero in both indices. The discrepancy between the two gamuts for the other illuminants is related systematically to correlated color temperature: redder lights score proportionally higher in our volume gamut than in Thornton's area gamut. In particular, tungsten light (Illuminant A) scores higher than most fluorescent and mercury lights. In contrast, Thornton's gamut area for tungsten light is about the same as the gamut areas for various mercury lamps and only half the area for standard daylight (Illuminant C).

Illuminating engineers are aware that "warmer" colored lights (with lower color

temperatures) are preferable in most applications, and our gamut reflects this preference. The high-pressure sodium lamp also scores quite high in our gamut rating, but achieves exceedingly poor rendition of color prints.

In the course of calculating these gamuts, we became interested in finding out which of the artist pigments are limit colors under the different illuminants. This information might assist artists in determining which colors are most important for their palettes. For example, in the pointillist style of painting,⁹ any color can be produced within a limit color solid by painting tiny dots of limit colors next to each other. When the observer stands back far enough the dots fuse and the colors mix additively.

Table XX-7 shows the subsets of limit colors that obtain with various illuminants, starting with the set of 37 artist pigments. We note that 10 pigments are always limit colors, 11 are always interior colors, and 16 switch according to the illuminant and the choice of color space. Pigments that are limit colors independent of illuminant are clearly of great importance in an artist's repertoire, for lighting under which a painting will be displayed cannot always be predicted. We note also that limit colors in Judd's space are almost always limit colors in Vos-Walraven space, and vice versa. Incidentally, it is demonstrable mathematically that the limit colors in Judd's space will be the same as those in any other CIE-derivable space.

Using Illuminant C, we ordered the artist limit pigments in their relative importance according to the fractional volume deficit incurred by removing each of them in turn from consideration. Two cases were considered. (i) The full set of 37 pigments was entered in the computation, thereby allowing possible new limit colors to replace the one that was removed. (ii) Only the 21 limit colors for Illuminant C were used.

The resultant ordering of the limit pigments according to volume deficit is shown in Table XX-8A. There are 4 cases in which removing a pigment causes a new limit color to emerge; in each such case, we enclose by parentheses the fractional volume deficit that results from using only the set of 21 limit colors. In Table XX-8, we order the limit colors by using a color space in which the green coordinate (which approximates luminance) is logarithmic, in accordance with the Weber-Fechner law.

4. Color Gamut Theory and the Energy Crisis

As a final endeavor, we considered theoretically the problem of augmenting the color gamut of the high-pressure sodium lamp, which has a very high luminous efficiency, by adding two spectral lines of given total energy. This might be useful in designing a lighting system with a fixed and adequate luminance level and a variable color rendering capability. Spectral characteristics of the theoretical lamps that best augment Thornton's gamut area and our gamut volume (in Judd space) are given in Table XX-9. Note that whereas optimizing Thornton's gamut requires the addition of blue and green lines, optimizing our gamut requires the addition of blue and red lines. Evidently this

Table XX-7. Identification of the limit artist pigments for 9 illuminants: Judd space, labeled O; Vos-Walraven space, labeled X.

Pigment	Illuminant									Limit Colors Always		
	MG	C	PC	DF	DM	A	WW	Na	GF			
1. Blue Verditer	O X										<u>Limit Colors Always</u> 1. Alizarin Crimson 2. Black (3% reflecting) 3. Cadmium Orange Medium 4. Cadmium Red 5. Chrome Yellow Medium 6. Emerald Green 7. French Ultramarine Blue 8. Red Lead 9. Verdigris 10. White	
2. Cadmium Yellow	O X	O X	O X	O X	O X	O X	O X	O X	O X			
3. Carmine Lake*	O X	O X	O X	O X	O X	O X	O	O X	O X	O X		
4. Chrome Green Medium*	O X	O X	O	O X	O	O X	O X	O X	O X			
5. Cobalt Blue	O X	O X	O X	O X	O X	O X	O X	O X	O X			
6. Cobalt Violet†									X	O X		
7. Dragon's Blood†					O X		X					
8. English Vermilion	O X	O X	O X		O X	O X	O X	O X	O X	O X		<u>Interior Colors Always</u> 1. Burnt Sienna 2. Cerulean Blue 3. Cobalt Green 4. Cobalt Yellow 5. Manganese Violet 6. Orpiment 7. Raw Sienna 8. Saffron 9. Ultramarine 10. Venetian Red 11. Yellow Ochre
9. Hansa Yellow	O X	O X	O X	O X	O X	O X	O X	O X	O X			
10. Indian Yellow	O X	O X	O X	O X	O X	O X	O X	O X	O X			
11. Madder Lake	O X	O X	O X	O X	O X	O X	O X	O X	O X			
12. Malachite										O X		
13. Smalt†	O X	O X	O X	O X	O X		O X			X		
14. Strontium Lemon Yellow	O X	O X	O X	O X	O X	O X	O X	O X	O X			
15. Viridian	O X	O X	O X	O X	O X	O X	O X	O X	O X			
16. Zinc Yellow*	O X		O	O	O X		O					

Notes: Symbols for illuminants same as in Table XX-6.

* Limit pigment in Judd space but not in Vos-Walraven space.

† Limit pigment in Vos-Walraven space but not in Judd space.

Table XX-8. Ordering of limit pigments under Illuminant C, according to the fractional volume deficits incurred on the limit solid by removing them. If V_0 is the volume of the limit solid before a given pigment is removed, and V is the volume afterward, then the fractional volume deficit is defined as $(V-V_0)/V_0$. Nonlimit pigments that become limit pigments when a given limit pigment is removed and fractional volume deficits that occur when these interior points have been previously discarded are in parenthesis.

A. Ordering in Vos-Walraven Space		B. Ordering in Vos-Walraven Space with a Logarithmic Green Coordinate	
Pigment	Log Space	Pigment	Log Space
	Fractional Volume Deficit (%)		Fractional Volume Deficit (%)
1. Emerald Green	16.5	1. Emerald Green	11.6
2. Madder Lake	7.8	2. Madder Lake	8.4
3. Cobalt Blue (Cerulean Blue, Blue Verditer)	4.4 (6.8)	3. Cobalt Blue (Cerulean Blue, Blue Verditer)	4.6 (7.0)
4. Chrome Yellow Medium	4.0	4. Chrome Yellow Medium	2.4
5. Verdigris	1.04	5. Verdigris	1.85
6. Red Lead	1.01	6. Smalt	1.36
7. Strontium Lemon Yellow (Zinc Yellow)	0.68 (5.9)	7. Red Lead	1.16
8. Smalt	0.47	8. French Ultramarine Blue	1.04
9. Cadmium Orange Medium	0.45	9. Black (3% reflecting) (Dragon's Blood)	0.93 (1.15)
10. Hansa Yellow	0.43	10. Alizarin Crimson	0.70
11. Black (3% reflecting) (Dragon's Blood)	0.31 (0.39)	11. Cadmium Orange Medium	0.53
12. French Ultramarine Blue	0.30	12. Hansa Yellow	0.36
13. Chrome Green Medium	0.25	13. Chrome Green Medium	0.32
14. Cadmium Yellow	0.24	14. Strontium Lemon Yellow (Zinc Yellow)	0.32 (2.9)
15. Alizarin Crimson	0.20	15. Viridian	0.13
16. Viridian	0.06	16. English Vermilion	0.12
17. English Vermilion	0.06	17. Cadmium Yellow	0.11
18. Indian Yellow	0.06	18. Indian Yellow	0.07
19. Carmine Lake (Dragon's Blood)	0.02 (0.02)	19. Cadmium Red	0.05
20. Cadmium Red	0.02	20. Carmine Lake (Dragon's Blood)	0.04 (0.06)

Table XX-9. Best color gamuts obtainable by adding 2 spectral lines of given total energy to the high-pressure sodium lamp.

Energy Fraction of Added Spectral Lines (%)	Dominant Wavelengths	Relative Energy at Each Wavelength	Thornton's Gamut Area $\times 2 \times 10^4$	$10^4 \times$ Volume Gamut in Judd Space	Gamut Maximized by Light
			Munsell Pigments	Munsell Pigments	
0	Light not Added to Na		18	57	
10	440 nm	.3	30	64	Volume Gamut in Judd Space Munsell Pigments
	640	.7			
20	440	.3		72	
	620	.7			
20	440	.9	61	63	Thornton's Gamut Area
	520	.1			

is due to the different color adaptation properties of the two spaces. An experiment to determine which of the sodium booster lamps is most effective is under consideration.

References

1. Dorothy Nickerson and C. W. Jerome, "Color Rendering of Light Sources: CIE Method of Specification and Its Application," *Illumin. Engrg.* 60, 262-271 (1965).
2. D. B. Judd, "A Flattery Index for Artificial Illuminants," *Illumin. Engrg.* 62, 593-598 (1967).
3. W. A. Thornton, "Color-Discrimination Index," *J. Opt. Soc. Am.* 62, 191-194 (1972).
4. J. von Kries, "Influence of Adaptation on the Effects Produced by Luminous Stimuli," *Handbuch der Physiologie des Menschen*, Vol. 3 (Vieweg, Brunswick, 1905), in D. L. MacAdam (Ed.), *Sources of Color Science* (The M.I.T. Press, Cambridge, Mass., 1970), pp. 120-126.
5. E. H. Land and J. J. McCann, "Lightness and Retinex Theory," *J. Opt. Soc. Am.* 61, 1-11 (1971).
6. D. B. Judd, "Standard Response Functions for Protanopic and Deuteranopic Vision," *J. Opt. Soc. Am.* 35, 199-221 (1945).
7. J. J. Vos and P. L. Walraven, "On the Derivation of the Foveal Receptor Primaries," *Vision Res.* 11, 799-818 (1970).
8. N. F. Barnes, "Color Characteristics of Artists' Pigments," *J. Opt. Soc. Am.* 29, 208-214 (1939).
9. W. C. Fleming, "Art," in *Encyclopedia Britannica*, Vol. 2 (William Benton, Chicago, 1969), see p. 488 for definition of pointillism.

(XX. NEUROPHYSIOLOGY)

D. IMPROVED LIGHT DIFFUSER BASED ON THE KALLIROSCOPE EFFECT

Bell Telephone Laboratories, Inc. (Grant)

Bradford Howland

[The research reported here was conducted while the author was a staff member of Lincoln Laboratory, M. I. T., and a research affiliate at the Research Laboratory of Electronics.]

In view of the energy crisis, it is important to consider all factors that could lead to improved efficiency of illumination, whether sunlight or electricity is used. In particular, some of the new high-efficiency illuminants such as mercury vapor or high-pressure sodium lamps, because of their very high luminosity, will require efficient light diffusers to reduce their specific brightness to a physiologically tolerable level.

An important property of a light diffuser is its ratio of forward-to-backward transmission, since light that is scattered backward into a light fixture, of necessity, will be partially absorbed. Certain rear projection screens have been optimized for this effect. Opal glass, which can be formed into a wide variety of luminary shapes, is the preferred solution in less critical applications, despite the fact that it often scatters more light backward than forward.

We shall describe an improved light-diffusing substance that transmits in sheet form 8 times more light in the forward than in the backward direction, and can be produced from inexpensive materials by ordinary manufacturing methods. The new light diffuser is based on the Kalliroscope effect invented by Paul Matisse (Kalliroscope Corporation, Cambridge, Massachusetts), in which myriads of small platelets of high refractive index are suspended in a fluid of similar density but lower index of refraction. In the Kalliroscope the alignment of these platelets is controlled by either the shear induced by fluid flow or the application of an electric field.

Substituting a polymerizable plastic for the suspending fluid and applying an electric field, we are able to create a "frozen" Kalliroscope pattern in which the axes normal to the planes of the platelets are oriented predominantly in the plane of a sheet of diffusing material. The effect is to create a sheet of composite uniaxial diffusing plastic with the following desirable properties: good diffusion of light, very high forward transmission with an inherently low light loss, and close-to-radial symmetry in the exiting light beam.

In Fig. XX-5 we show the method of manufacture of a sample of this plastic. In order to monitor the casting operation, we use two glass plates with semitransparent gold-conducting inner surfaces spaced approximately 1/8 inch apart. These plates are coated with a mold-release agent (polyvinyl alcohol) and are electrically connected to a 110-volt, 60-cycle source through a Variac. The polymerizing solution is prepared

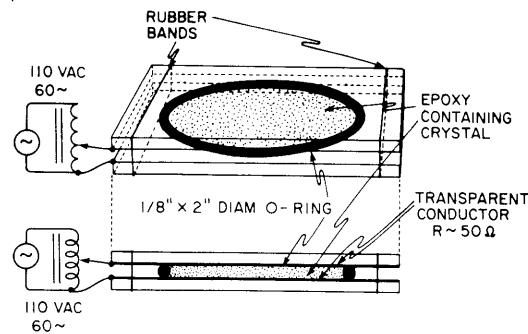


Fig. XX-5. Arrangement of conducting glass plates and O-ring that contains the mixture of clear plastic and hexagonal platelets (pearly pigment) during the hardening phase.

as follows: First a catalyzed mixture of clear plastic, Maraset #657 A and B (The Marabette Corporation, Long Island City, New York) is prepared and centrifuged to remove bubbles. With this we mix a variable fraction (a few percent) of Type ZHP, A-6891, Nacromer pearly pigment (The Mearle Corporation, New York) which consists of a suspension of lead carbonate hexagonal platelets in xylene. The mixture is poured between the conducting plates and is contained by the O-ring. Alignment of the particles is indicated by the electric field-induced transparency of the plastic and is achieved a few seconds after application of 110 V. The polymerized mixture is a good conductor, however, and so the voltage must be reduced immediately to the minimum (~ 30 V) that will maintain transparency during several hours of curing time; otherwise thermal effects will wreck the specimen.

Because of the voltage reduction, the alignment of the axes of the platelets in the plane of the diffuser is less than perfect. This, in fact, enhances the effectiveness of the diffuser up to a point.

Figure XX-6 shows the geometry of rays entering the plastic mixture at an external angle ϕ , corresponding to an internal angle ϵ , both measured with respect to the normal to the surface of the diffuser. The effect of multiple reflections from the oriented platelets, because of the mismatch in refractive indices of platelet and medium, with diffraction neglected, is preservation of angle ϵ with respect to the normal while the azimuthal internal angle of the light beam is rotated by some random amount. Since many such reflections occur, the effect is to homogenize the beam thoroughly about the azimuthal angles. That is, the exiting beam may be described as a cone of light having an apex angle 2ϕ with considerable broadening by diffraction at the small ($25 \mu\text{m}$) apertures of the hexagonal platelets and by the random misalignments of the axes of these platelets. This predicted behavior is realized in practice. A weak mixture of platelets shows the predicted conical exiting beam with a strong directly transmitted ray. A concentrated

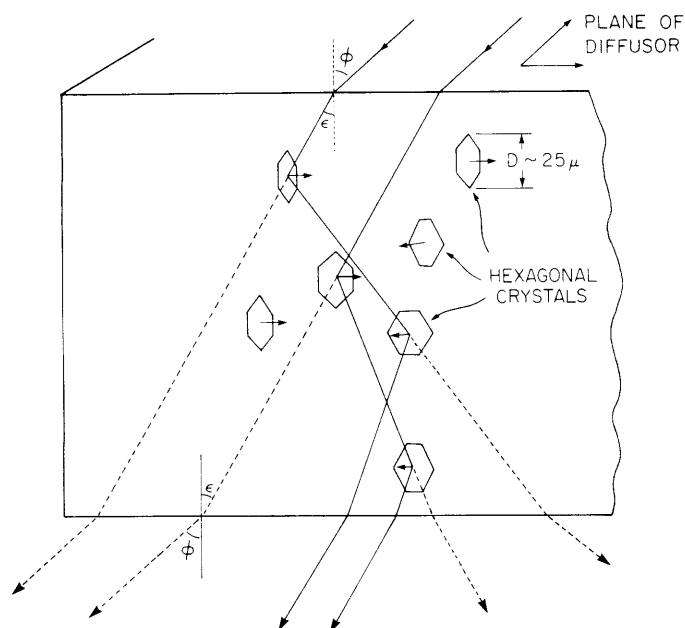


Fig. XX-6. Cross section of the new diffuser, with tracings of typical light rays to show mode of action. The size of the platelets ($25 \mu\text{m}$ diameter) is greatly exaggerated. Refractive indices of plastic and platelets are 1.52 and 2.09.

mixture of platelets in clear plastic shows a nearly radial symmetric exiting beam in which the cone of light is largely filled in. In particular, and this is the most important point, there is no mechanism for backscatter of light, except for specular reflections at the surfaces of the diffuser.

Figure XX-7 shows polar plots of the behavior of a sample of the new diffusing material, and for comparison a sample of opal glass (Edmund Scientific Company, Barrington, New Jersey) for two orientations of the entering light. The ratio of forward-to-backward transmission for the new diffuser in each case is approximately 8:1, while for the opal glass it is slightly less than unity. For the new diffuser, the exiting beam has a half-width of approximately 60° for the normally incident illumination and 80° for illumination 30° off normal. For most purposes, this is an adequate degree of diffusion.

The present diffusing substance, we believe, has considerable potential once the problems of mass production have been mastered, since it would have application to lighting fixtures and to window diffusers, where the high forward-to-backward ratio is an important advantage. Another possible variation in performance could be obtained by the induction of a viscous shear between the plates very near the end of the hardening phase after the alignment voltage has been switched off. This would result in obtaining a diffuser with an optical axis that would no longer be normal to the surface and could

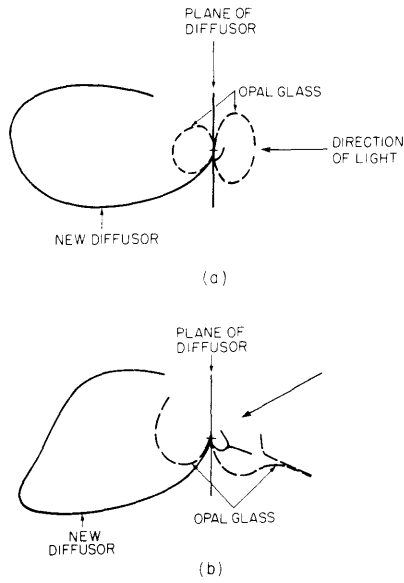


Fig. XX-7.

Polar diagrams comparing the light transmission as a function of angle for the new diffuser (solid lines) and opal glass (dotted lines). (a) Incident light normal to the surface. (b) Incident light 30° off the normal.

have important applications in redirection of sunlight or for attenuation of sunlight at unfavorable angles, particularly with the addition of a second component of absorbing platelets. Finally, we point out that the cost and availability of the ingredients, casting resin and pearlite crystals, is unlikely to be the controlling factor in the cost of manufacture of this product.

